

Sequential vector and axial-vector meson exchange and chiral loops in radiative phi decay

J. E. Palomar, L. Roca, E. Oset and M. J. Vicente Vacas

Departamento de Física Teórica and IFIC, Centro Mixto Universidad de Valencia-CSIC,
Institutos de Investigación de Paterna, Aptdo. 22085, 46071 Valencia, Spain

March 25, 2022

Abstract

We study the radiative ϕ decay into $\pi^0\pi^0\gamma$ and $\pi^0\eta\gamma$ taking into account mechanisms in which there are two sequential vector-vector-pseudoscalar or axial-vector-vector-pseudoscalar steps followed by the coupling of a vector meson to the photon, considering the final state interaction of the two mesons. There are other mechanisms in which two kaons are produced through the same sequential mechanisms or from ϕ decay into two kaons and then undergo final state interaction leading to the final pair of pions or $\pi^0\eta$, this latter mechanism being the leading one. The results of the parameter free theory, together with the theoretical uncertainties, are compared with the latest experimental results of KLOE at Frascati.

1 Introduction

The radiative decays of the ϕ into $\pi^0\pi^0\gamma$ and $\pi^0\eta\gamma$ have been the subject of intense study [1, 2, 3, 4, 5, 6, 7]. One of the main reasons for this is the hope that one can get much information about the nature of the $f_0(980)$ and $a_0(980)$ resonances from the invariant mass distribution of the two mesons. The nature of the scalar meson resonances has generated a large debate [8], to which new light has been brought by the claim that these resonances are dynamically generated from multiple scattering with the ordinary chiral Lagrangians [9, 10, 11].

These two reactions involving the decay of the ϕ are special. Indeed, the ϕ does not decay into two pions because of isospin symmetry. A way to circumvent this handicap is to allow the ϕ to decay into two charged kaons (with a photon attached to one of them) and the two kaons to scatter giving rise to the two pions (or $\pi^0\eta$). The loop which appears diagrammatically is proved to be finite using arguments of gauge invariance [12, 13, 5]. The radiative ϕ decay through this mechanism was studied in [5] and the results of lowest order chiral perturbation theory (χPT) were used to account for the $K^+K^- \rightarrow \pi^0\pi^0$ transition.

Since the chiral perturbation theory $K^+K^- \rightarrow \pi^0\pi^0$ amplitude does not account for the $f_0(980)$, the excitation of this resonance has to be taken in addition, something that has been done more recently using a linear sigma-model in [14].

The work of [7] leads to the excitation of the $f_0(980)$ in the $\pi^0\pi^0$ production, or the $a_0(980)$ in $\pi^0\eta$ production in a natural way, since the use of unitarized chiral perturbation theory ($U\chi PT$), as in [9], generates automatically those resonances in the meson meson scattering amplitudes and one does not have to introduce them by hand.

The experimental situation has also experienced an impressive progress recently. To the already statistically significant experiments at Novosibirsk [15, 16, 17] one has added the new, statistically richer, experiments at Frascati [18, 19] which allow one to test models beyond the qualitative level. In this sense although the predictions of the work of [7], using $U\chi PT$ with no free parameters, provided a good agreement with the experimental data of [15, 16, 17], thus settling the dominant mechanism as that coming from chiral kaon loops from the $\phi \rightarrow K^+K^-$ decay, the new and more precise data leave room for finer details which we evaluate in this paper.

One of the issues concerning radiative decays is the relevance of the sequential vector meson mechanisms. The anomalous vector-vector-pseudoscalar couplings [20, 21], followed by the coupling of the photon to the vector mesons through vector meson dominance, allows mechanisms for reactions of the type that we study, through a sequential $V \rightarrow VP \rightarrow PP\gamma$ process. This mechanism is known to provide the $\omega \rightarrow \pi^0\pi^0\gamma$ radiative width with accuracy [21] and has been further extended to study $\rho \rightarrow \pi^0\pi^0\gamma$ and other radiative decays in [22, 23]. In particular, it was found that in the latter reaction the sequential vector meson mechanism and the loops (in this case charged pion loops) were equally important, and the consideration of the two mechanisms produced a width compatible with the recent experimental determination of the SND collaboration [24]. Since the $\phi \rightarrow \rho\pi^0$ is OZI forbidden, the contribution from the sequential vector meson mechanism should be small and it was not considered till recently [25, 6]. It proceeds via $\phi - \omega$ mixing, which is indeed small, but still noticeable in the radiative ϕ decay width.

In the present paper we also take into account this sequential mechanism, but in addition we consider the final state interaction of the two mesons within the framework of $U\chi PT$. Furthermore, in the line of considering the final state interaction (FSI) of the mesons we also allow the sequential vector meson production of kaons, which interact among themselves and lead to the final two mesons. This is easily implemented in the coupled channel formalism of [9]. The mechanisms involving final state interaction all contribute to the production of the $f_0(980)$ or $a_0(980)$ resonances, since the resonance poles appear in the coupled channel formalism in all the elastic or transition matrix elements.

Another novelty of the present work is the consideration of sequential mechanisms involving the exchange of an intermediate axial-vector meson ($J^{PC} = 1^{++}$ or 1^{+-}), both producing directly the final meson pair or through the intermediate production of kaons which undergo collisions and produce these mesons.

All the mechanisms considered here contribute moderately, but appreciably, to the ϕ radiative width. The inclusion of all these mechanisms leads to results compatible with the experimental data of Frascati, particularly if theoretical uncertainties are considered,

which is something also done in the present work.

The good agreement with experiment is reached in spite of having in our approach a width for the $f_0(980)$ very small, of the order of 30 MeV, seemingly in contradiction with the 'visual' $f_0(980)$ width in the experiment, which looks much larger. The reason for this has been recently discussed in [26,27] and stems from the fact that, due to gauge invariance, the amplitude for the process contains as a factor the momentum of the photon, which grows fast as we move down to smaller invariant masses of the two pseudoscalars from the mass of the $f_0(980)$ where the photon momentum is very small. This distorts the shape of the resonance, making it appear wider. We shall see that our approach, which respects gauge invariance, introduces automatically this factor in the amplitudes.

We shall see that there is some discrepancy of the theoretical results with the data at small two meson invariant masses. We shall discuss this feature, realizing that the results resemble very much the raw data, before the analysis is done to subtract the contribution of $\omega\pi^0$ and to correct for the experimental acceptance. Furthermore, some of the assumptions made in the analysis of [18] might be questionable.

2 The $\phi \rightarrow \pi^0\pi^0\gamma$ decay

2.1 Kaon loops from $\phi \rightarrow K^+K^-$ decay

The mechanism for radiative decay using the tensor formulation for the vector mesons has been discussed in [28,7] and we briefly summarize it here. The diagrams considered are depicted in Fig. 1, where the loops contain K^+K^- . The vertices needed for the diagrams are obtained from the chiral Lagrangian

$$\mathcal{L} = \frac{F_V}{2\sqrt{2}} \langle V_{\mu\nu} f_+^{\mu\nu} \rangle + \frac{iG_V}{\sqrt{2}} \langle V_{\mu\nu} u^\mu u^\nu \rangle, \quad (1)$$

where the notation is defined in [29]. We also assume ideal mixing between the ϕ and the ω

$$\sqrt{\frac{2}{3}}\omega_1 + \frac{1}{\sqrt{3}}\omega_8 \equiv \omega \quad , \quad \frac{1}{\sqrt{3}}\omega_1 - \frac{2}{\sqrt{6}}\omega_8 \equiv \phi \quad (2)$$

and the matrix V is then given by

$$V_{\mu\nu} \equiv \begin{pmatrix} \frac{1}{\sqrt{2}}\rho_{\mu\nu}^0 + \frac{1}{\sqrt{2}}\omega_{\mu\nu} & \rho_{\mu\nu}^+ & K_{\mu\nu}^{*+} \\ \rho_{\mu\nu}^- & -\frac{1}{\sqrt{2}}\rho_{\mu\nu}^0 + \frac{1}{\sqrt{2}}\omega_{\mu\nu} & K_{\mu\nu}^{*0} \\ K_{\mu\nu}^{*-} & \bar{K}_{\mu\nu}^{*0} & \phi_{\mu\nu} \end{pmatrix} \quad (3)$$

The amplitude for the radiative decay can be written as $T^{\mu\nu}\epsilon_\mu(\gamma)\epsilon_\nu(\phi) \equiv t$, and Lorentz covariance demands $T^{\mu\nu}$ to be of the type

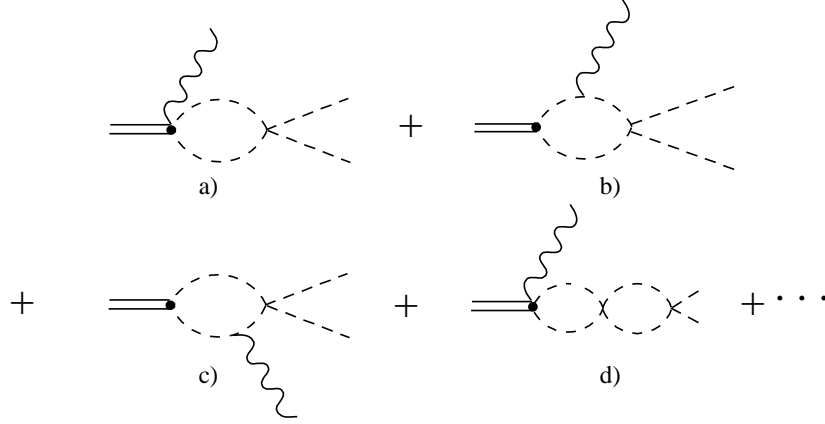


Figure 1: Loop diagrams included in the chiral loop contributions. The intermediate states in the loops are K^+K^- .

$$T^{\mu\nu} = a g^{\mu\nu} + b P^\mu P^\nu + c P^\mu q^\nu + d P^\nu q^\mu + e q^\mu q^\nu \quad (4)$$

where P, q are the ϕ and photon momenta respectively. Gauge invariance ($q_\nu T^{\mu\nu} = 0$) forces $b = 0$ and $d = -a/(P \cdot q)$. If one works in the Coulomb gauge only the $g^{\mu\nu}$ term of Eq. (4) contributes which is calculated from the d term to which only the diagrams b), c) of Fig. 1 contribute. Since two powers of momenta correspond to $P^\nu q^\mu$ the loop integrals with the remaining momenta are actually convergent [12, 13]. Furthermore, if the $K^+K^- \rightarrow \pi^0\pi^0$ amplitude is separated into the on shell part (setting $p^2 = m^2$ for the internal lines) and the off shell remainder, it was proved in [30] that this latter part does not contribute to the d coefficient. This information is of much value, since it allows to factorize the on shell meson meson amplitude outside the loop integral. The amplitude for the process is given by

$$t = -\sqrt{2} \frac{e}{f^2} \epsilon(\phi) \cdot \epsilon(\gamma) \left[M_\phi G_V \tilde{G}(M_I) + q \left(\frac{F_V}{2} - G_V \right) G(M_I) \right] t_{K^+K^-, \pi^0\pi^0} \quad (5)$$

where $f = 92.4$ MeV and \tilde{G} is the convergent loop function of [12, 13] given by

$$\begin{aligned} \tilde{G}(M_\phi, M_I) &= \frac{1}{8\pi^2} (a - b) I(a, b) \\ a &= \frac{M_\phi^2}{m^2}; \quad b = \frac{M_I^2}{m^2} \end{aligned} \quad (6)$$

where m is the mass of the meson in the loop, M_I the invariant mass of the two mesons and $I(a, b)$ accounts for the three meson loop and is given analytically in Eq. (12) of [30]. On the other hand, $G(M_I)$ is the ordinary loop function of two meson propagators which appears in the study of the meson meson interaction in [9] and which is regularized there

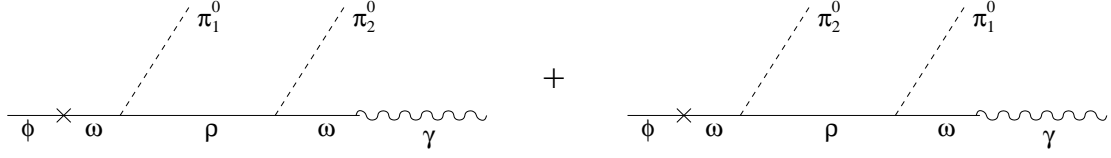


Figure 2: Diagrams for the tree level VMD mechanism.

with a cut off of the order of 1 GeV. In Eq. (5) the $t_{K^+K^-, \pi^0\pi^0} = \frac{1}{\sqrt{3}} t_{K\bar{K}, \pi\pi}^{I=0}$ is the transition amplitude with the iterated loops implicit in the coupled channels Bethe Salpeter equation (BS) obtained in [9]. The parameters F_V , G_V , for the vector mesons are obtained from their decay into e^+e^- , $\mu^+\mu^-$ or two mesons. If one works at the tree level one finds $F_V^{(\rho)} = 153 \pm 2$ MeV from $\rho \rightarrow e^+e^-$ or $F_V^{(\rho)} = 143 \pm 5$ MeV from $\rho \rightarrow \mu^+\mu^-$ decay. On the other hand, from $\pi^+\pi^-$ decay at tree level one finds $G_V^{(\rho)} = 69$ MeV or if one meson loop is considered $G_V^{(\rho)} = 55$ MeV [29]. Similarly for the ϕ one finds $F_V^{(\phi)} = 161 \pm 2$ MeV from $\phi \rightarrow e^+e^-$ or $F_V^{(\phi)} = 151 \pm 6$ MeV from $\phi \rightarrow \mu^+\mu^-$. From $\phi \rightarrow K^+K^-$ decay at tree level we find $G_V^{(\phi)} = 55$ MeV but this value would be 5% higher from $\phi \rightarrow K^0\bar{K}^0$. It is interesting to recall that when the iteration of loops implicit in the BS equation is used to evaluate pion and kaon electromagnetic form factors in [31] one finds a universal value for $G_V = 55$ MeV and similarly $F_V = 154$ MeV. Since here we use a similar formalism to the one used in [31] the use of this latter values of the constants according to the approach used gives us an indication of the level of uncertainty in these parameters. We thus take for the calculations $F_V = 156 \pm 5$ MeV and $G_V = 55 \pm 5$ MeV.

2.2 Sequential vector meson exchange mechanisms

Following the lines of [22, 23] in the study of ρ and ω radiative decays and the more recent of [25, 6] in the ϕ decay, we also include these mechanisms here. They are depicted in Fig. 2, where we explicitly assume that the $\phi \rightarrow \rho^0\pi^0$ proceeds via the $\phi - \omega$ mixing.

In order to evaluate these diagrams we use the same Lagrangians as in [5, 22]

$$\begin{aligned}\mathcal{L}_{VVP} &= \frac{G}{\sqrt{2}} \epsilon^{\mu\nu\alpha\beta} \langle \partial_\mu V_\nu \partial_\alpha V_\beta P \rangle \\ \mathcal{L}_{V\gamma} &= -4f^2 eg A_\mu \langle Q V^\mu \rangle\end{aligned}\quad (7)$$

where $\langle \rangle$ means $SU(3)$ trace, $g = -4.41$, $G = \frac{3g^2}{4\pi^2 f} = 0.016$ MeV $^{-1}$, $Q = \text{diag}\{2/3, -1/3, -1/3\}$, V (P) the vector (pseudoscalar) $SU(3)$ matrices and e is taken positive.

In addition we must use the Lagrangians producing the ϕ - ω mixing. We use the formalism of [32]

$$\mathcal{L}_{\phi\omega} = \Theta_{\phi\omega} \phi_\mu \omega^\mu \quad (8)$$

which means that the diagrams of Fig. 2 can be evaluated assuming the decay of the ω (with mass M_ϕ) multiplying the amplitude by $\tilde{\epsilon}$ (the measure of the ϕ - ω mixing) given by

$$\tilde{\epsilon} = \frac{\Theta_{\phi\omega}}{M_\phi^2 - M_\omega^2} \quad (9)$$

Values of $\Theta_{\phi\omega}$ of the order of 20000 – 29000 MeV² are quoted in [33] which are compatible with $\tilde{\epsilon} = 0.059 \pm 0.004$ used in [34]¹ which is the value used here.

The amplitude for the $\phi(q^*) \rightarrow \pi_1^0(p_1)\pi_2^0(p_2)\gamma(q)$ decay corresponding to the diagrams of Fig. 2 is given by

$$t = -C\tilde{\epsilon}\frac{2\sqrt{2}egf^2G^2}{3M_\omega^2} \left[\frac{P^2\{a\} + \{b(P)\}}{M_\rho^2 - P^2 - iM_\rho\Gamma_\rho(P^2)} + \frac{P'^2\{a\} + \{b(P')\}}{M_\rho^2 - P'^2 - iM_\rho\Gamma_\rho(P'^2)} \right] \quad (10)$$

where $P = p_2 + q$, $P' = p_1 + q$ and

$$\begin{aligned} \{a\} &= \epsilon^* \cdot \epsilon \, q^* \cdot q - \epsilon^* \cdot q \, \epsilon \cdot q^* \\ \{b(P)\} &= -\epsilon^* \cdot \epsilon \, q^* \cdot P \, q \cdot P - \epsilon \cdot P \, \epsilon^* \cdot P \, q^* \cdot q + \epsilon^* \cdot q \, \epsilon \cdot P \, q^* \cdot P + \epsilon \cdot q^* \, \epsilon^* \cdot P \, q \cdot P \end{aligned} \quad (11)$$

with ϵ^* and ϵ the polarization vectors of the ϕ and the photon respectively.

At this point it is worth mentioning that the theoretical expression for the $V \rightarrow P\gamma$ decay widths $\Gamma_{V \rightarrow P\gamma} = \frac{4}{3}\alpha C_i^2 \left(\frac{Ggf^2}{M_\rho M_V}\right)^2 k^3$, with C_i the $SU(3)$ coefficients given in Table I of [36] obtained from the Lagrangians of Eq. (7), gives slightly different results to the experimental values from [37]. For this reason we can follow a similar procedure to that used for the $\eta \rightarrow \pi^0\gamma\gamma$ decay in [36] where the C_i coefficients were normalized so that the theoretical $V \rightarrow P\gamma$ decay widths agree with experiment. In the $\phi \rightarrow \pi^0\pi^0\gamma$ reaction this procedure results in including in Eq. (10) a normalizing factor $\mathcal{C} = 0.869 \pm 0.014$, obtained considering the $V \rightarrow P\gamma$ reactions shown in Table I of [36].

2.3 Pion final state interaction in the sequential vector meson mechanism

Since the $\pi\pi$ interaction is strong in the region of invariant masses relevant in the present reaction we next consider the final state interaction of the pions in the sequential vector meson mechanism.

We must take into account the loop function of Fig. 3a, but on the same footing we must also consider those of Fig. 3b and 3c, where charged pions are produced and allowed to interact to produce the $\pi^0\pi^0$ final state. The thick dot in Fig. 3 means that one is considering the full $\pi\pi \rightarrow \pi\pi$ t-matrix, involving the loop resummation of the BS equation of ref. [9] and not just the lowest order $\pi\pi \rightarrow \pi\pi$ amplitude.

In order to evaluate those diagrams we must calculate the loop function with a ρ and two pion propagators. First let us note that due to isospin symmetry the $\omega\rho^0\pi^0$ coupling

¹Note that in [21] a different sign for $\tilde{\epsilon}$ is claimed. This is actually a misprint and the results of that paper are calculated with $\tilde{\epsilon} > 0$ [35].

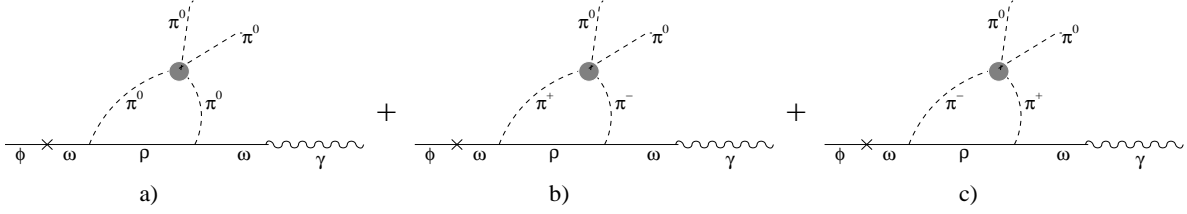


Figure 3: VMD diagrams with final state interaction of pions

is the same as the $\omega\rho^+\pi^-$ or $\omega\rho^-\pi^+$. Next, given the structure of the terms in Eqs. (10) and (11) we must evaluate the loop integrals

$$i \int \frac{d^4 P}{(2\pi)^4} P^\mu P^\nu \frac{1}{P^2 - M_V^2 + i\epsilon} \frac{1}{(q^* - P)^2 - m_1^2 + i\epsilon} \frac{1}{(q - P)^2 - m_2^2 + i\epsilon} \quad (12)$$

For simplicity we evaluate these integrals in the reference frame where the two meson system has zero momentum. In this frame the ϕ and photon trimomentum are the same, \vec{q} . We need the following integrals, which for dimensional reasons we write as

$$\begin{aligned} i \int \frac{d^4 P}{(2\pi)^4} P^0 P^0 D_1 D_2 D_3 &= I_0 \\ i \int \frac{d^4 P}{(2\pi)^4} P^0 P^i D_1 D_2 D_3 &= \frac{q^i}{|\vec{q}|} I_1 \\ i \int \frac{d^4 P}{(2\pi)^4} P^i P^j D_1 D_2 D_3 &= \delta_{ij} I_a + \frac{q^i q^j}{q^2} I_b \end{aligned} \quad (13)$$

where D_1, D_2, D_3 are the three meson propagators of Eq. (12). The integrals are evaluated in the Appendix. For that purpose the P^0 integral is evaluated analytically and the $d^3 \vec{P}$ integral is evaluated numerically by means of the same cut off which has been used to regularize the two meson loop in the meson meson interaction, i.e., a cut off of the order of 1 GeV.

The amplitude is then written as

$$t = -C\tilde{\epsilon} \frac{2\sqrt{2} egf^2 G^2}{3 M_\omega^2} \epsilon^* \cdot \epsilon q \left\{ I_a (2q^{*0} - q) + I_b q^{*0} + I_0 q - I_1 (q^{*0} + q) \right\} 2t_{\pi\pi, \pi\pi}^{I=0} \quad (14)$$

where

$$q = \frac{M_\phi^2 - M_I^2}{2M_I} \quad , \quad q^{*0} = M_I + q = \frac{M_\phi^2 + M_I^2}{2M_I}. \quad (15)$$

Note that, since we evaluate the amplitudes in the Coulomb gauge and $\vec{\epsilon}$ is transverse to \vec{q} , $\vec{\epsilon}$ is not modified by a boost connecting the two meson system and the ϕ rest frame. The same thing happens to $\vec{\epsilon}^*$

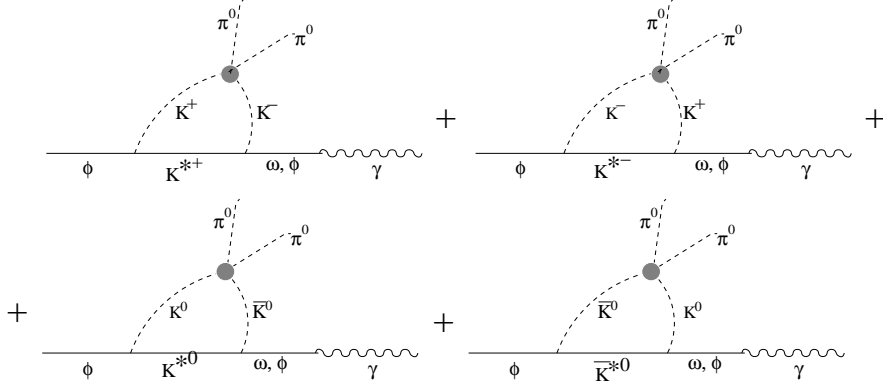


Figure 4: VMD diagrams with final state interaction of kaons

Thus the invariant t matrix of Eq. (14) is evaluated with the polarizations in the ϕ rest frame, like the amplitude in sections 2.1 and 2.2. The function multiplying $\epsilon^* \cdot \epsilon$, which is thus invariant, is evaluated in the rest frame of the two mesons, as we have done.

In Eq. (14) we have also taken into account that

$$\langle \pi^0 \pi^0 + \pi^+ \pi^- + \pi^- \pi^+ | t | \pi^0 \pi^0 \rangle = 2t_{\pi\pi, \pi\pi}^{I=0} \quad (16)$$

where $t_{\pi\pi}^{I=0}$ is the $I = 0$ $\pi\pi$ scattering amplitude in the unitary normalization of the states used in [9]. Note that we have used the prescription in which the $\pi\pi$ scattering amplitude is factorized on shell in the loops and this is justified in [9] for the loops implicit in the BS equation, in [30] for the loops of Fig. 1, as we mentioned before, and in [38] for looping diagrams of the type of those we are now discussing. Note also that we take only the s-wave part of the $\pi\pi \rightarrow \pi\pi$ scattering amplitude, the p-wave part for $\pi^0 \pi^0$ being forbidden. Anticipating results, we should mention that in the case of $\pi^0 \eta$ in the final state we shall also use only the s-wave scattering amplitude since the p-wave part is zero at lowest order χPT and negligible if higher orders are considered [39].

2.4 Kaon loops in the sequential vector meson mechanisms

Next we consider the diagrams analogous to those in Fig. 3 but with kaons in the intermediate states.

Note that unlike in sections 2.2 and 2.3 the ϕVP vertices are now not OZI forbidden. They come from the Lagrangian of Eq. (7). All the four ϕKK^* vertices in Fig. 4 have the same strength and taking into account the $\omega\gamma$, $\phi\gamma$ couplings coming from Eq. (7) we obtain for the set of diagrams of Fig. 4

$$t = -\mathcal{C} \frac{egf^2 G^2}{3} \epsilon^* \cdot \epsilon q \left\{ I_a(2q^{*0} - q) + I_b q^{*0} + I_0 q - I_1(q^{*0} + q) \right\}. \quad (17)$$

$$\cdot \frac{4}{\sqrt{3}} t_{K\bar{K},\pi\pi}^{I=0} \left(\frac{1}{M_\omega^2} - \frac{2}{M_\phi^2} \right)$$

where the I_i integrals are now evaluated using K , \bar{K} and K^* in the three meson loop. In Eq. 17 we have used that

$$\langle K^+ K^- + K^- K^+ + K^0 \bar{K}^0 + \bar{K}^0 K^0 | t | \pi^0 \pi^0 \rangle = \frac{4}{\sqrt{3}} t_{K\bar{K},\pi\pi}^{I=0} \quad (18)$$

with $t_{K\bar{K},\pi\pi}^{I=0}$ the $I = 0$ $K\bar{K} \rightarrow \pi\pi$ unitarized transition amplitude evaluated with the states with the unitary normalization of [9]. Unlike in the case of pion loops where only the ω is attached to the photon, now we can have the ω and the ϕ without violating the OZI rule. The two terms in the last factor of Eq. (17) account for the ω and ϕ meson respectively.

2.5 Sequential axial vector meson mechanisms

Since the mass of the ϕ is around 250 MeV higher than the ρ mass, and we are considering sequential vector meson mechanisms with ρ or K^* exchange, we should pay attention to the analogous mechanisms involving vector mesons with a similar mass difference with the ϕ on the upper side and these are the axial and vector mesons with $J^{PC} = 1^{+-}$ or 1^{++} (see Table 1). Therefore, the b_1 or a_1 axial vector mesons and the K_{1B} , K_{1A} strange axial vector mesons will play the role of the ρ or the K^* in former diagrams.

J^{PC}	$I = 1$	$I = 0$	$I = 1/2$
1^{+-}	$b_1(1235)$	$h_1(1170), h_1(1380)$	K_{1B}
1^{++}	$a_1(1260)$	$f_1(1285), f_1(1420)$	K_{1A}

Table 1: Octets of axial-vector mesons.

Because of the C parity of the states, the Lagrangians for the axial-vector-vector-pseudoscalar couplings have the structure of $\langle B\{V, P\} \rangle$ for the b_1 octet and $\langle A[V, P] \rangle$ for the octet of the a_1 [40], where the $\langle \rangle$ means $SU(3)$ trace. In the last expressions V and P are the usual vector and pseudoscalar $SU(3)$ matrices respectively and

$$B \equiv \begin{pmatrix} \frac{1}{\sqrt{2}} h_1(1170) + \frac{1}{\sqrt{2}} b_1^0 & b_1^+ & K_{1B}^+ \\ b_1^- & \frac{1}{\sqrt{2}} h_1(1170) - \frac{1}{\sqrt{2}} b_1^0 & K_{1B}^0 \\ K_{1B}^- & \bar{K}_{1B}^0 & h_1(1380) \end{pmatrix}$$

$$A \equiv \begin{pmatrix} \frac{1}{\sqrt{2}} f_1(1285) + \frac{1}{\sqrt{2}} a_1^0 & a_1^+ & K_{1A}^+ \\ a_1^- & \frac{1}{\sqrt{2}} f_1(1285) - \frac{1}{\sqrt{2}} a_1^0 & K_{1A}^0 \\ K_{1A}^- & \bar{K}_{1A}^0 & f_1(1420) \end{pmatrix}. \quad (19)$$

In addition one has to consider an approximate 50 % mixture of the K_{1B} and K_{1A} states to give the physical $K_1(1270)$ and $K_1(1400)$ states [42, 41, 40].

We have modified the original Lagrangian of [40] to treat the vector fields in the tensor formalism of [29]. This formalism has the advantage that without basically changing the rates of the $A \rightarrow VP$ decays, one deduces the coupling of the a_1 to $\pi\gamma$ using vector meson dominance through $a_1 \rightarrow \pi\rho \rightarrow \pi\gamma$, with an amplitude which is gauge invariant and which is in agreement with the chiral structure of [29] for the $a_1 \rightarrow P\gamma$ couplings and with the experiment. Details are given elsewhere in [43].

We hence use the Lagrangians [43]

$$\begin{aligned}\mathcal{L}_{BVP} &= \tilde{D} < B_{\mu\nu} \{V^{\mu\nu}, P\} > \\ \mathcal{L}_{AVP} &= i\tilde{F} < A_{\mu\nu} [V^{\mu\nu}, P] >\end{aligned}\tag{20}$$

where the i factor in front of the \tilde{F} is needed in order \mathcal{L}_{AVP} to be hermitian.

In Eq. (20) the fields $W_{\mu\nu} \equiv A_{\mu\nu}$, $B_{\mu\nu}$ are normalized such that

$$< 0 | W_{\mu\nu} | W; P, \epsilon > = \frac{i}{M_W} [P_\mu \epsilon_\nu(W) - P_\nu \epsilon_\mu(W)]\tag{21}$$

In addition the propagators with the tensor fields are defined as [29]

$$\begin{aligned}< 0 | T \{ W_{\mu\nu} W_{\rho\sigma} \} | 0 > = i\mathcal{D}_{\mu\nu\rho\sigma} = \\ &= i \frac{M_W^{-2}}{M_W^2 - P^2 - i\epsilon} [g_{\mu\rho} g_{\nu\sigma} (M_W^2 - P^2) + g_{\mu\rho} P_\nu P_\sigma - g_{\mu\sigma} P_\nu P_\rho - (\mu \leftrightarrow \nu)]\end{aligned}\tag{22}$$

The physical $K_1(1270)$ and $K_1(1400)$, with a mixture around 45 degrees ² found in [42, 41, 40, 43], can be expressed, in terms of the $I = 1/2$ members of the $1^{+-}(1^{++})$ octets, $K_{1B}(K_{1A})$, as

$$\begin{aligned}K_1(1270) &= \frac{1}{\sqrt{2}}(K_{1B} - iK_{1A}) \\ K_1(1400) &= \frac{1}{\sqrt{2}}(K_{1B} + iK_{1A})\end{aligned}\tag{23}$$

With the values for $\tilde{D} = -1000 \pm 120 \text{ MeV}$ and $\tilde{F} = 1550 \pm 150 \text{ MeV}$, very similar to those found in [42, 41, 40], we are able to describe all the $A \rightarrow VP$ decays plus the radiative decays of the $a_1 \rightarrow \pi\gamma$ [43].

Once again the ϕ sequential decay at tree level through b_1 exchange is OZI violating and proceeds via $\phi - \omega$ mixing. We have evaluated this contribution and found it negligible, thus we do not further discuss it. Similarly the loops involving pions are equally negligible. On the other hand a_1 exchange is not allowed by C and G parity.

²It is worth mentioning that in [42, 43] two more possible solutions for the mixing angle around 30 and 60 degrees were found. This uncertainty will be taken into account in the evaluation of the error band in our final results.

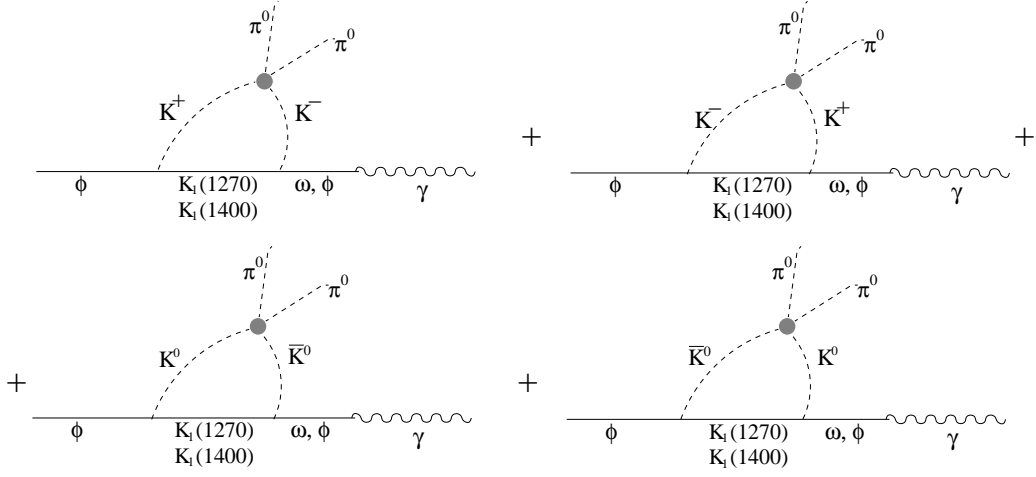


Figure 5: Diagrams for the sequential mechanisms involving the K_1 axial-vector mesons.

2.6 Kaon loops from sequential axial vector meson mechanisms

The relevant mechanisms involving axial-vectors are those in Fig. 5 in which K , \bar{K} are created and through scattering lead to the final $\pi^0\pi^0$ state. These are not OZI forbidden and have a nonnegligible contribution.

Since we are using the tensor formulation for the vector mesons this forces us to use the tensor coupling of the photon to the vector mesons obtained from the F_V term of Eq. (1):

$$\mathcal{L}_{V\gamma} = -e \frac{F_V}{2} \lambda_V V_{\mu\nu}^0 (\partial^\mu A^\nu - \partial^\nu A^\mu) \quad (24)$$

with $\lambda_V = 1, \frac{1}{3}, -\frac{\sqrt{2}}{3}$ for $V = \rho, \omega, \phi$ respectively.

Now the amplitude with $K_1(1270)$ as intermediate state is given, following the lines of sections 2.3 and 2.4 as

$$t = \frac{4eF_V}{M_\phi M_{K_1}^2} \epsilon^* \cdot \epsilon \frac{4}{\sqrt{3}} t_{K\bar{K},\pi\pi}^{I=0} \left[\frac{(\tilde{D}^2 - \tilde{F}^2)}{6\sqrt{2}M_\omega^2} - \frac{\sqrt{2}(\tilde{D} + \tilde{F})^2}{6M_\phi^2} \right] \cdot q \left[q^{*0} I_0 + I_a(2q - q^{*0}) + I_b q - I_1(q + q^{*0}) + (q - q^{*0}) G_{K\bar{K}}(M_I) \right]_{K_1 \equiv K_1(1270)} \quad (25)$$

The amplitude for the diagram with intermediate $K_1(1400)$ is the same as Eq. (25) but replacing \tilde{F} by $-\tilde{F}$ and using the $K_1(1400)$ propagator in the evaluation of the I_i integrals.

The term proportional to $G_{K\bar{K}}(M_I)$ at the end of the former expression comes from the $M_{K_1}^2 - P^2$ of Eq. (22) which cancels the intermediate vector meson propagator, thus leaving the loop with just two pseudoscalar propagators, which is the same one that appears in the meson meson scattering.

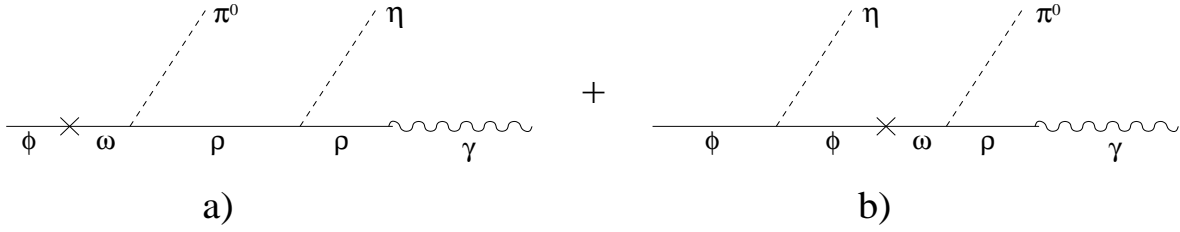


Figure 6: Diagrams for the tree level VMD mechanism for the $\phi \rightarrow \pi^0 \eta \gamma$ decay.

3 The $\phi \rightarrow \pi^0 \eta \gamma$ decay

After the discussion of the former points the consideration of the $\phi \rightarrow \pi^0 \eta \gamma$ decay requires only minimal technical details which we write below.

3.1 Kaon loops from $\phi \rightarrow K \bar{K}$ decay.

The diagrams to be considered are exactly the same as those in Fig. 1 changing the final $\pi^0 \pi^0$ by $\pi^0 \eta$. Technically all that we do is to substitute in Eq. (5) the amplitude $t_{K^+ K^-, \pi^0 \pi^0}$ by the $t_{K^+ K^-, \pi^0 \eta}$ or equivalently $-\frac{1}{\sqrt{2}} t_{K \bar{K}, \pi^0 \eta}^{I=1}$ in the nomenclature of [9].

3.2 Sequential vector meson contribution

We have now the diagrams

The amplitude of this contribution is very similar to Eq. (10). We find

$$t = -\mathcal{C}\tilde{\epsilon} \frac{4}{\sqrt{3}} \frac{egf^2 G^2}{M_\rho^2} \left\{ \frac{P^2 \{a\} + \{b(P)\}}{M_\rho^2 - P^2 - iM_\rho \Gamma_\rho(P^2)} - \frac{P'^2 \{a\} + \{b(P')\}}{M_\phi^2 - P'^2 - iM_\phi \Gamma_\phi(P'^2)} \right\} \quad (26)$$

3.3 $\pi \eta$ final state interaction of the sequential vector meson mechanism

The results for the amplitude corresponding to FSI in diagram 6a is easily obtained from Eq. (14). We multiply the expression by $\sqrt{6}$, change the masses and widths of the corresponding intermediate particles in the loops and change $2t_{\pi\pi, \pi\pi}^{I=0}$ by $t_{\pi\eta, \pi\eta}^{I=1}$. The amplitude corresponding to the FSI in diagram 6b is done in the same way but we multiply by $-\sqrt{6}$ instead of $\sqrt{6}$ to account for the negative sign in Eq. (26).

3.4 Kaon loops from sequential vector meson mechanisms

The diagrams involved are the same as in Fig. 4 but instead of ω and ϕ coupled to the photon we have now only the ρ and the final $\pi^0 \pi^0$ is substituted by $\pi^0 \eta$. Altogether one must change $\frac{1}{M_\omega^2}$ to $\frac{1}{M_\rho^2}$ in the ω term of Eq. (17) and substitute $t_{K \bar{K}, \pi\pi}^{I=0}$ by $-3\sqrt{\frac{3}{2}} t_{K \bar{K}, \pi\eta}^{I=1}$.

3.5 Axial vector meson exchange mechanisms

The tree level with b_1 , a_1 exchange and their octet partners are also OZI forbidden and negligible like in the case of $\pi^0\pi^0$ final state. However, the term with kaon loops equivalent to Fig. 5 but with $\pi^0\eta$ in the final state and a ρ coupled to the photon instead of ω , ϕ are OZI allowed and we take them into account.

Once again the amplitude is easily obtained from that of the ω part of Eq. (25) by changing $\frac{1}{M_\omega^2}$ to $\frac{1}{M_\rho^2}$ and $t_{K\bar{K},\pi\pi}^{I=0}$ to $-\frac{3\sqrt{3}}{\sqrt{2}}t_{K\bar{K},\pi\eta}^{I=1}$ and the same considerations regarding the contribution of the $K_1(1270)$ and $K_1(1400)$ intermediate states.

4 Results

4.1 Differential cross section

Using the transition amplitudes described in the previous sections, we can calculate the differential decay widths of the ϕ meson as,

$$\frac{d\Gamma}{dM_I} = \frac{1}{64\pi^3} \int_{m_\pi}^{M_\phi - q - m'} d\omega \frac{M_I}{M_\phi^2} \bar{\sum} \sum |t|^2 \Theta(1 - \cos^2 \theta_{\pi^0\gamma}), \quad (27)$$

where M_I is the invariant mass of the final two mesons, m' is the pion mass for the $\pi\pi\gamma$ decay and the η mass for the $\pi\eta\gamma$ decay and q is the photon momentum in the initial ϕ rest frame. Θ is the step function and $\theta_{\pi^0\gamma}$ accounts for the angle between the π^0 and the photon and it is given by

$$\cos^2 \theta_{\pi^0\gamma} = \frac{1}{2pq} \left[(M_\phi - \omega(p) - q)^2 - m'^2 - p^2 - q^2 \right], \quad (28)$$

where p and $\omega(p)$ are the π^0 momentum and energy in the initial ϕ rest frame. A symmetry factor 1/2 must be implemented in Eq. (27) in the case of $\pi^0\pi^0$ in the final state.

The spin sum and average of the transition amplitudes, $\bar{\sum} \sum |t|^2$, can be expressed using the contravariant tensor F^{ij} as:

$$\bar{\sum} \sum |t|^2 = \frac{1}{3} \left[F^{ij} F^{ij*} - \frac{1}{|q|^2} (F^{ij} q_j) (F^{ij'*} q_{j'}) \right], \quad (29)$$

where the tensor expression F^{ij} of the transition amplitude t is defined as

$$t \equiv F^{ij} \epsilon_i(V) \epsilon_j(\gamma). \quad (30)$$

4.2 Results for the $\phi \rightarrow \pi^0\pi^0\gamma$ decay

First of all, we show in Fig. 7 the contribution of the chiral loops (solid line) together with the sequential VMD mechanisms at tree level of Fig. 2 (dotted line) and the VMD with final state interaction, Fig. 3, (dashed line). In the dashed-dotted line we have plotted the

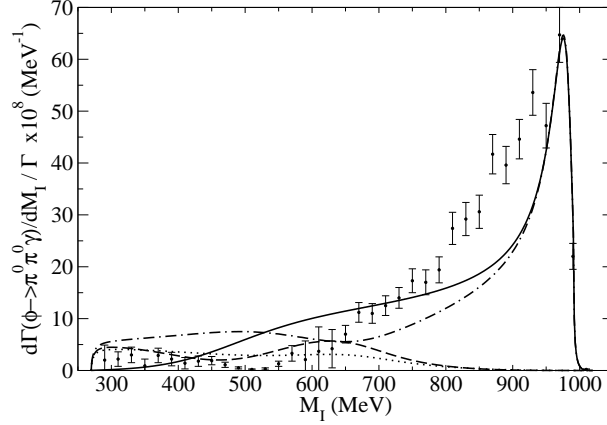


Figure 7: Several contributions to the $\pi^0\pi^0$ invariant mass distribution for the $\phi \rightarrow \pi^0\pi^0\gamma$ decay. Solid line: chiral loops of Fig. 1. Dotted line: sequential VMD at tree level of Fig. 2. Dashed line: sequential VMD including the FSI of Fig. 3. Dashed-dotted line: Coherent sum of all these mechanisms. (Experimental data from [18]).

contribution of all these mechanisms together. We can see, that the effect of the VMD tree level contribution and its unitarization is small compared to the chiral loops from $\phi \rightarrow K^+K^-$ decay. The total contribution is still rather different than the experimental values of [18], although the inclusion of the sequential vector meson mechanism provides some strength for the distributions at low invariant masses where the kaon loops from $\phi \rightarrow K^+K^-$ are negligible.

In Fig. 8 we can see the contribution of the sequential mechanisms involving kaon loops (Fig. 4), separating the ϕ (dashed line) and ω (dashed-dotted line) contributions, and the coherent sum of both amplitudes (solid line). We can see that the sum of both mechanisms almost cancels, thus making the contribution of the kaon loops of the sequential VMD mechanisms very small, although the individual contribution of the loops with an ω or a ϕ meson attached to the photon are sizeable when they interfere separately with the chiral loops from $\phi \rightarrow K^+K^-$ decay, as it can be seen in Fig. 9. Had this accidental cancellation not happened the contribution of the kaon loops of the sequential mechanisms would have been sizeable.

In Fig. 10 we show the contribution of the axial-vector meson resonances. We can see the contribution of the mechanisms with a $K_1(1270)$ as intermediate state (dashed line) and the one with $K_1(1400)$ (solid line) (see Fig. 5). The size of these mechanisms by themselves is very small but when they interfere with the chiral loops from $\phi \rightarrow K^+K^-$ decay they give an important contribution, as shown in Fig. 11. Thus, these mechanisms with the axial-vector mesons in the intermediate states cannot be neglected.

In Fig. 12 we show the contribution of the different relevant mechanisms as they have been added to the model. In the dashed line we can see the contribution of the chiral

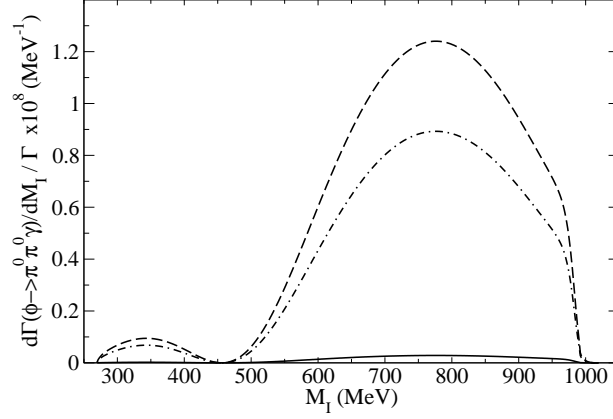


Figure 8: Contribution of the sequential mechanisms involving kaon loops. Dashed line: ϕ contribution. Dashed-dotted line: ω contribution. Solid line: Coherent sum of ϕ and ω contributions.

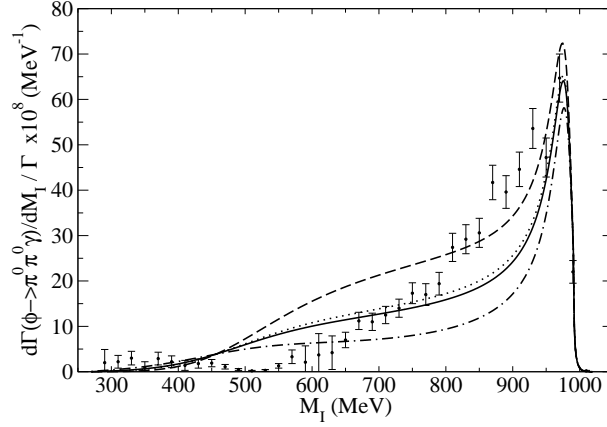


Figure 9: Addition of the sequential loops contribution to the chiral loops of Fig. 1. Solid line: chiral loops of Fig. 1. Dashed line: chiral loops of Fig. 1 + sequential loops involving kaons with ϕ . Dashed-dotted line: chiral loops of Fig. 1 + sequential loops involving kaons with ω . Dotted line: Coherent sum of all these contributions.

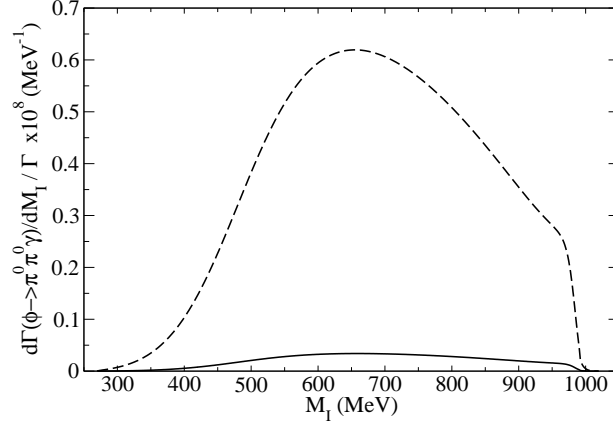


Figure 10: Contribution of the sequential mechanisms involving axial-vector mesons. Solid line: $K_1(1270)$ contribution. Dashed line: $K_1(1400)$ contribution.

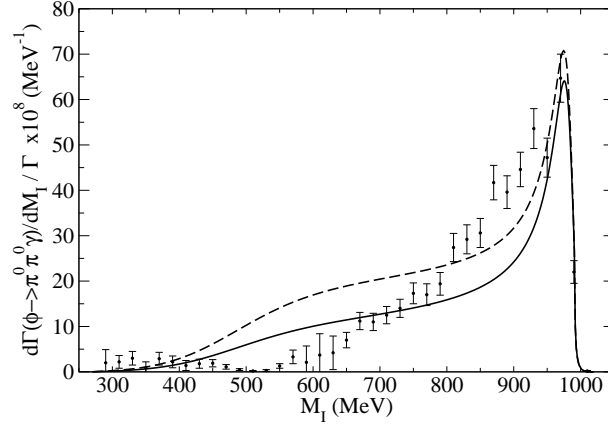


Figure 11: Addition of the sequential loops involving axial-vector mesons to the chiral loops of Fig. 1. Solid line: chiral loops of Fig. 1. Dashed line: chiral loops of Fig. 1 + axial-vector meson contribution.

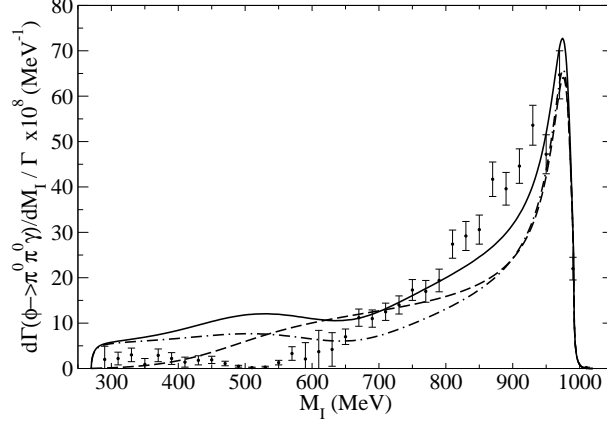


Figure 12: Different contributions to the two pion invariant mass distributions of the $\phi \rightarrow \pi^0 \pi^0 \gamma$ decay: Dashed line: chiral loops of Fig. 1. Dashed-dotted line: chiral loops of Fig. 1 + sequential VMD and its final state interaction. Solid line: idem plus the contribution of the mechanisms involving axial-vector mesons, (full model).

\mathcal{C}	$\tilde{\epsilon}$	G_V (MeV)	F_V (MeV)
0.869 ± 0.014	0.059 ± 0.004	55 ± 5	156 ± 5
f_π (MeV)	Λ (MeV)	\tilde{D} (MeV)	\tilde{F} (MeV)
$92.4 \pm 3\%$	1000 ± 50	-1000 ± 120	1550 ± 150

Table 2: Parameters which uncertainties are relevant in the error analysis. The f_π and Λ are the f_π constant and cutoff of the momentum integral respectively in the loops involved in the unitarized meson-meson rescattering.

loops. In the dashed-dotted line we add the contribution of the sequential VMD and its final state interaction. In the solid line we add the contribution of the loops of the sequential mechanisms with axial-vector mesons in the intermediate states. This latter line represents the full model.

Up to now, all the curves shown in the figures have been calculated using the central values of the parameters without considering the uncertainties in their values. In Fig. 13 we show the final result but including an evaluation of the error band due to the uncertainties in the parameters of the model. This error band has been calculated implementing a Monte Carlo gaussian sampling of the parameters within their experimental errors. The parameters of the model which uncertainties are relevant in the error analysis are shown in Table 2.

The errors in f_π and Λ assumed in the calculations have been chosen such that the quality of the fit to the $\pi\pi$ phase shifts along the lines of [9] is still acceptable within

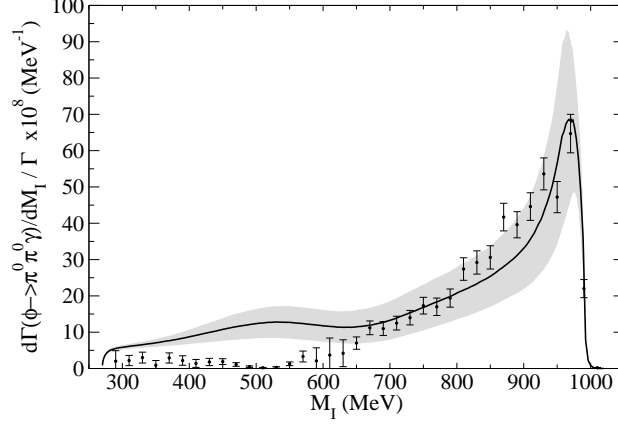


Figure 13: Final results for the $\pi^0\pi^0$ invariant mass distribution for the $\phi \rightarrow \pi^0\pi^0\gamma$ decay with the theoretical error band. Experimental data from [18].

experimental errors.

The parameter with the larger contribution to the error band turns out to be the G_V since the largest contribution, chiral kaon loops form $\phi \rightarrow K^+K^-$ decay, is roughly proportional to G_V (up to the term with $q(\frac{F_V}{2} - G_V)$ in Eq. (5) which would be zero within some vector meson dominance hypotheses [29] and is small with our set of parameters).

The total width and branching ratio obtained in the present work are

$$\begin{aligned} \Gamma_{\phi \rightarrow \pi^0\pi^0\gamma} &= 520 \pm 150 \text{ eV} \\ BR(\phi \rightarrow \pi^0\pi^0\gamma) &= (1.2 \pm 0.3) \times 10^{-4} \end{aligned} \quad (31)$$

to be compared with the experimental values

$$BR^{exp}(\phi \rightarrow \pi^0\pi^0\gamma) = (1.22 \pm 0.10 \pm 0.06) \times 10^{-4} \quad [15]$$

$$BR^{exp}(\phi \rightarrow \pi^0\pi^0\gamma) = (0.92 \pm 0.08 \pm 0.06) \times 10^{-4} \quad [16]$$

$$BR^{exp}(\phi \rightarrow \pi^0\pi^0\gamma) = (1.09 \pm 0.03 \pm 0.05) \times 10^{-4} \quad [18]$$

In Fig. 13 we can see that our results, considering the error band, fairly agree with the experimental data except in the region around 500 MeV. The reason of this discrepancy will be further discussed in Section 5.

4.3 Results for the $\phi \rightarrow \pi^0\eta\gamma$ decay

In Fig. 14 we show the contribution of the chiral loops from $\phi \rightarrow K^+K^-$ decay (dashed-dotted line) together with the sequential VMD at tree level (dotted line) and the loops of

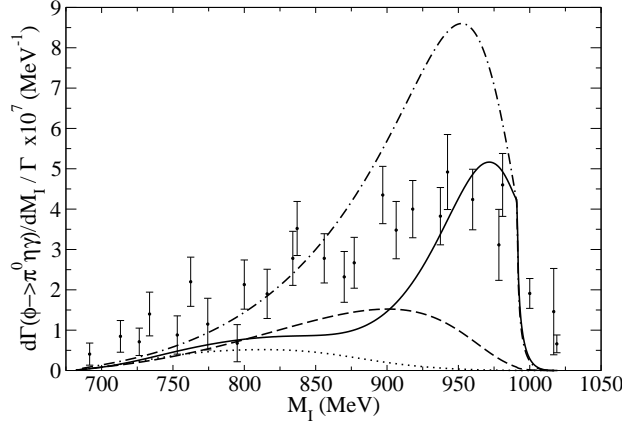


Figure 14: Several contributions to the $\pi^0\eta$ invariant mass distribution of the $\phi \rightarrow \pi^0\eta\gamma$ decay. Dashed-dotted line: chiral loops of Fig. 1. Dotted line: sequential VMD at tree level. Dashed line: loops of the sequential VMD involving kaons. Solid line: coherent sum of all these mechanisms. (Experimental data from [25]).

the sequential VMD involving kaons (dashed line). In the solid line we show the coherent sum of all these contributions.

In this case the VMD mechanism involving $\pi\eta$ creation followed by $\pi\eta \rightarrow \pi\eta$ FSI is negligible and, therefore, is not shown in the figure. We can see that the kaon loops of the sequential VMD mechanism give a very important contribution, in contrast to the $\phi \rightarrow \pi^0\pi^0\gamma$ case where the important contribution of the VMD sequential loops was the one involving pions. Recall that the reason for the small contribution of kaon loops in the VMD mechanism for $\phi \rightarrow \pi^0\pi^0\gamma$ was the accidental cancellation of the ϕ and ω contributions (for the ϕ and ω attached to the photon). However, in this case there is only the ρ attached to the photon and thus the contribution of this term is large, as was also the case in $\phi \rightarrow \pi^0\pi^0\gamma$ for the individual contributions.

In Fig. 15 we show the contribution of the mechanisms with intermediate $K_1(1270)$ (solid line) and $K_1(1400)$ (dashed line).

These contributions by themselves are very small but when they interfere with the chiral loops give a sizeable contribution, (from dashed to solid line in Fig. 16).

In Fig. 17 we show the different relevant contributions when they are added one by one.

The dotted line represents the chiral loops by themselves. In the dashed line we have added the contribution of the sequential VMD mechanisms together with the loops involving the FSI of the mesons. Finally, in solid line we have add the contribution of the axial-vector contributions. This latter curve represents the full model. In this figure we can see the importance of the loop mechanism involving kaons and the nonnegligible contribution of the mechanisms with axial-vector mesons in intermediate states.

Again, in Fig. 18 we have plotted the full model performing the theoretical error analy-

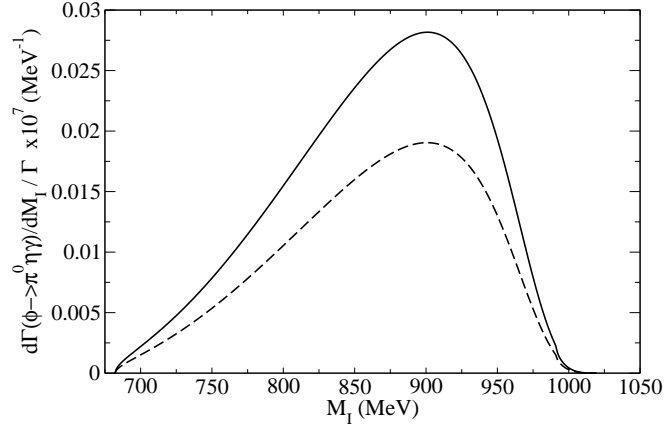


Figure 15: Contribution of the sequential mechanisms involving axial-vector mesons. Solid line: $K_1(1270)$ contribution. Dashed line: $K_1(1400)$ contribution.

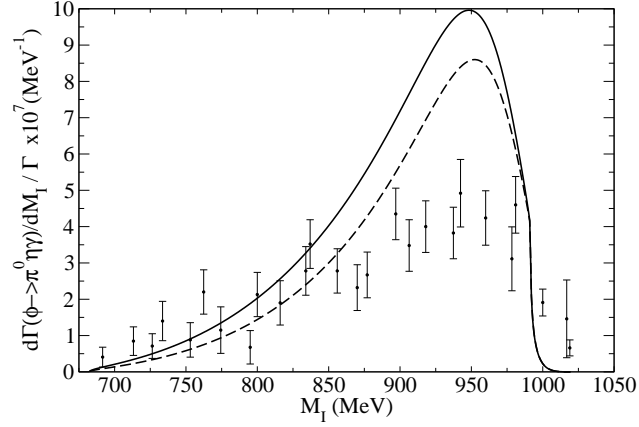


Figure 16: Addition of the sequential loops involving axial-vector mesons to the chiral loops of Fig. 1. Solid line: chiral loops of Fig. 1. Dashed line: chiral loops of Fig. 1 + axial-vector meson contribution.

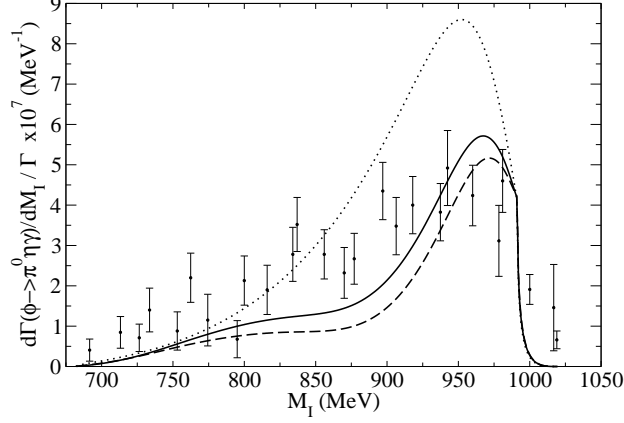


Figure 17: Different contributions to the $\pi^0\eta$ invariant mass distributions of the $\phi \rightarrow \pi^0\eta\gamma$ decay: Dotted line: chiral loops of Fig. 1. Dashed line: chiral loops of Fig. 1 + sequential VMD and its final state interaction. Solid line: idem plus the contribution of the mechanisms involving axial-vector mesons, (full model).

sis³. We can see that when these uncertainties are considered we obtain a theoretical band in acceptable agreement with the experimental data.

The total width and branching ratio obtained are

$$\begin{aligned}\Gamma_{\phi \rightarrow \pi^0\eta\gamma} &= 250 \pm 80 \text{ eV} \\ BR(\phi \rightarrow \pi^0\eta\gamma) &= (0.59 \pm 0.19) \times 10^{-4}\end{aligned}\tag{32}$$

to be compared with the experimental values

$$BR^{exp}(\phi \rightarrow \pi^0\eta\gamma) = (0.88 \pm 0.14 \pm 0.09) \times 10^{-4} \quad [17]$$

$$BR^{exp}(\phi \rightarrow \pi^0\eta\gamma) = (0.90 \pm 0.24 \pm 0.10) \times 10^{-4} \quad [16]$$

$$BR^{exp}(\phi \rightarrow \pi^0\eta\gamma) = (0.85 \pm 0.05 \pm 0.06) \times 10^{-4} \quad [19]$$

5 Further discussion of the $\phi \rightarrow \pi^0\pi^0\gamma$ results.

We would like to comment on the strength that we obtain around 500 MeV in the $\pi^0\pi^0$ invariant mass distribution in the $\phi \rightarrow \pi^0\pi^0\gamma$ decay which appears in contradiction with

³We have also checked that the use of a mixing angle for the strange members of the axial nonets of around 30 or 60 degrees [42, 43] turns out in decreasing the lower limit of the error band in around 5% and 10% for the $\phi \rightarrow \pi^0\pi^0\gamma$ and $\phi \rightarrow \pi^0\eta\gamma$ decays respectively.

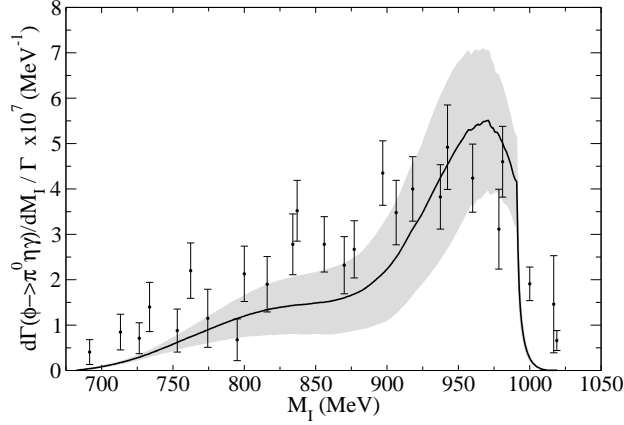


Figure 18: Final results for the $\pi^0\eta$ invariant mass distribution for the $\phi \rightarrow \pi^0\eta\gamma$ decay with the theoretical error band.

the experimental analysis. As we saw it comes from accumulation of the novel mechanisms which we have discussed in our paper. Such mechanisms are not considered in other theoretical papers which find a good agreement with the data. For instance in [6] a good reproduction of the data is obtained using a linear sigma model with $\sigma(500)$ and $f_0(980)$ included in the calculation and some free parameter to adjust to the data. In [27] an attempt to make a model independent calculation is done by parametrizing amplitudes compatible with analyticity and gauge invariance and, through a fit to data, a set of parameters leading to agreement with the data is obtained. In [44] the same approach for the chiral kaon loops from $\phi \rightarrow K^+K^-$ decay as in the present paper is followed, but in addition a contact term in $\phi\gamma K^0\bar{K}^0$ is added and, fitting the strength of this term to the data, a good agreement with the experimental results is also found. Our philosophy has been different and we have not fitted any parameter to the ϕ radiative decay data but simply have considered the different mechanisms that can sizeably contribute to the process. An acceptable agreement with the data is found in the region of the $f_0(980)$, which is the most important issue concerning this reaction. This is not trivial a priori in view of the very small width of the dynamically generated $f_0(980)$ (around 30 MeV) that one obtains in the model of [9] that we use here and the large 'visual' width of the $f_0(980)$ peak in the present experiment. Part of the reason for the agreement comes from the q factor (photon momentum) in the amplitude, as required by gauge invariance and emphasized in [26, 27], which gives more weight to the amplitude as we move down in the $\pi\pi$ invariant mass from the upper limit (where $q = 0$). However, as seen in our results, the inclusion of the new mechanisms and their interference with the dominant one, particularly the contribution of the axial-vector meson exchange mechanisms, also contributes to the widening of the distribution around the $f_0(980)$ peak.

Although the agreement with data at low masses is not very good, we must point out

two sources of uncertainty in the experimental spectrum. First, the results in the low and intermediate mass region largely depend on the background subtraction dominated by the non-resonant $\omega\pi^0$ process. The size of this process is difficult to obtain because it has a strong background itself, mostly from the $\phi \rightarrow f_0\gamma$ process, as it is discussed in [45]. There, its magnitude has been obtained in a model dependent way assuming some a priori spectrum for the $\phi \rightarrow f_0\gamma$ process [45]. In fact, before the subtraction, the raw data resemble much more our calculated spectrum, (see fig. 4 from [18]), and we could think of a slightly smaller $\omega\pi^0$ background.

Additionally, there is some uncertainty in the way the data are corrected to account for the experimental efficiency. This is done in [18] by dividing the observed spectrum by the effect of applying the experimental efficiency on some theoretical distribution. This unfolding procedure depends on the theoretical model used, which we think at low $\pi^0\pi^0$ masses is at least incomplete. In fact, with the unfolding method used, the zero value of the spectrum obtained with the theoretical model of [18] implies unavoidably a zero value for the corrected experimental results. A reanalysis to the light of the present discussion would be most welcome.

6 Conclusions

We have studied the radiative decay of the ϕ into two neutral pseudoscalars, $\pi^0\pi^0$, $\pi^0\eta$, and a photon. We have taken an approach to study the process addressing mechanisms proved to be relevant in the study of the radiative decays of the ρ and the ω . These include the kaon loops from the $\phi \rightarrow K^+K^-$ decay and mechanisms of sequential vector meson steps with vertices of the type VVP , together with vector meson dominance to couple a vector meson to the photon.

In addition to these mechanisms studied before we have added the final state interaction in the sequential vector meson mechanisms, allowing for rescattering of the $\pi^0\pi^0$ or $\pi^0\eta$ states. Simultaneously we also allowed kaons to be produced in the sequential vector meson processes, followed by the interaction of the kaons to lead to the final $\pi^0\pi^0$ or $\pi^0\eta$ states. These latter mechanisms have the advantage over the tree level sequential vector meson mechanism that they are not OZI forbidden. We found these kaon loop contributions to be individually large, although they become small in the $\phi \rightarrow \pi^0\pi^0\gamma$ decay due to an accidental cancellation of two terms, and they are very important in the $\phi \rightarrow \pi^0\eta\gamma$ decay.

Another addition in the present work is the contribution of sequential axial-vector mechanisms involving two sequential AVP steps followed by the coupling of a vector meson to the photon, and even more important the production of $K\bar{K}$ through these mechanisms followed by final state interaction of the kaons to give $\pi^0\pi^0$ or $\pi^0\eta$ in the final state.

The final state interaction of pairs of mesons involving diagrams with loops has been done using techniques of unitarized chiral perturbation theory which allow one to study meson meson interaction in coupled channels up to 1.2 GeV and hence are particularly suitable for the present reaction.

The main contribution to the radiative ϕ decay is the loop mechanisms involving the

interaction of K^+K^- coming from ϕ decay, which by itself reproduces qualitatively the experiment as it was already shown in [7]. However, the new mechanisms studied here are by no means negligible. Altogether we find a good agreement with experiment, particularly when the study of the theoretical uncertainties is done. These theoretical uncertainties, stemming from errors in the magnitudes used as input to determine the parameters of the theory, are of the same order of magnitude as the experimental ones. Apart from these uncertainties we should stress that there is no freedom in the theory used. There are no free parameters which have been adjusted to the $\phi \rightarrow \pi^0\pi^0\gamma$ and $\phi \rightarrow \pi^0\eta\gamma$ data studied here. The agreement with the experimental data both for $\pi^0\pi^0$ and $\pi^0\eta$ channel is remarkable and less than trivial when one realizes that a change of sign in one of the mechanisms leads to opposite interference effects and to results in not so good agreement with the data. The agreement is more remarkable, or surprising, when one realizes that this agreement with the data is reached for the $\pi^0\pi^0\gamma$ case, in spite of having an $f_0(980)$ resonance that has a width much smaller than the apparent width that one could guess from the $\phi \rightarrow \pi^0\pi^0\gamma$ experiment, and which one would get fitting the data with models less elaborate than the present one. Some explanation for this can be already seen in [26,27] which remarked that the requirement of gauge invariance in the amplitude introduces the factor of the photon momentum which tends to widen the distribution of the invariant mass around the $f_0(980)$ peak. Our approach is manifestly gauge invariant and one can show explicitly in all the terms that this factor appears. Our approach comes to stress the point of view of [26,27] that the apparent width of the $f_0(980)$ in the experimental data of this reaction can not be used as an direct measure of the actual $f_0(980)$ width.

The main conclusion of the work is that a theoretical approach to the problem of the $\phi \rightarrow \pi^0\pi^0\gamma$ and $\phi \rightarrow \pi^0\eta\gamma$ decays is possible by using the chiral unitary approach used successfully to reproduce the $\pi\pi$ data up to 1.2 GeV and many other physical processes [46]. As we could see along the work, the $f_0(980)$ or $a_0(980)$ have not been explicitly coupled to the ϕ , meaning that there is no direct $\phi \rightarrow f_0\gamma, a_0\gamma$ coupling. This is in accordance with the philosophy of the chiral unitary approach about these two resonances which are dynamically generated by the meson meson interaction. This has as a consequence that in processes where these resonances are produced one should not include them explicitly in the approach but they should appear naturally as soon as the meson are allowed to interact. In this sense the present work comes to reinforce the claim that the $f_0(980)$ and $a_0(980)$ are dynamically generated resonances and that the meson meson chiral Lagrangian at lowest order contains the driving forces that make possible this generation through the multiple scattering of the mesons in coupled channels.

Acknowledgments

Two of us, J.E.P. and L.R., acknowledge support from the Ministerio de Educación, Cultura y Deporte. This work is partly supported by DGICYT contract number BFM2000-1326, and the E.U. EURIDICE network contract no. HPRN-CT-2002-00311.

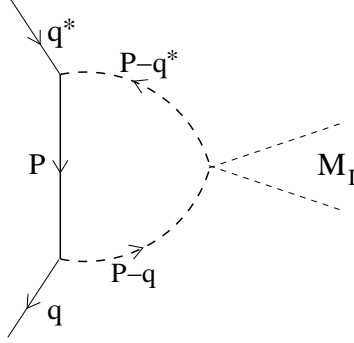


Figure 19: Three meson loop.

Appendix: Integrals involving three meson propagators

For the evaluation of the loop of Fig. 19 we need to calculate the integrals of Eq. (13). From Eq. (13) it is easy to obtain that

$$\begin{aligned}
 I_0 &= i \int \frac{d^4 P}{(2\pi)^4} P^0 P^0 D_1 D_2 D_3 \\
 I_1 &= i \int \frac{d^4 P}{(2\pi)^4} P^0 |\vec{P}| \cos \theta D_1 D_2 D_3 \\
 I_a &= \frac{i}{2} \int \frac{d^4 P}{(2\pi)^4} \vec{P}^2 \sin^2 \theta D_1 D_2 D_3 \\
 I_b &= \frac{i}{2} \int \frac{d^4 P}{(2\pi)^4} \vec{P}^2 (3 \cos^2 \theta - 1) D_1 D_2 D_3
 \end{aligned} \tag{33}$$

where $D_1 = \frac{1}{P^2 - M_V^2 + i\epsilon}$, $D_2 = \frac{1}{(P-q^*)^2 - m_1^2 + i\epsilon}$ and $D_3 = \frac{1}{(P-q)^2 - m_2^2 + i\epsilon}$.

Defining $\omega_V = \sqrt{\vec{P}^2 + M_V^2}$, $\omega_2 = \sqrt{(\vec{P} - \vec{q})^2 + m_2^2}$ and $\omega_1 = \sqrt{(\vec{P} - \vec{q}^*)^2 + m_1^2}$, the analytical structure in the complex P^0 plane of the integrals of Eqs. (33) is depicted in Fig. 20.

Applying the Residues Theorem with the path shown in Fig. 20, the evaluation of the P^0 integral gives

$$\begin{aligned}
 I_i &= \frac{1}{2} \int \frac{d \cos \theta d |\vec{P}|}{(2\pi)^2} \frac{|\vec{P}|^2}{\omega_1 \omega_2} \frac{\tilde{A}_i}{(q^{*0} + \omega_1 + \omega_V)(q^{*0} - \omega_1 - \omega_V + i \frac{\Gamma_V(s'_V)}{2})(q^{*0} - q^0 + \omega_1 + \omega_2 - i\epsilon)} \\
 &\quad \cdot \frac{1}{(q^0 + \omega_2 + \omega_V)(q^0 - \omega_2 - \omega_V + i \frac{\Gamma_V(s_V)}{2})(q^0 - q^{*0} + \omega_1 + \omega_2 - i\epsilon)} \tag{34}
 \end{aligned}$$

for $i = \{0, 1, a, b\}$, with $s_V = (q^{*0} - \omega_1)^2 - \vec{P}^2$, $s'_V = (q^0 - \omega_2)^2 - \vec{P}^2$ and

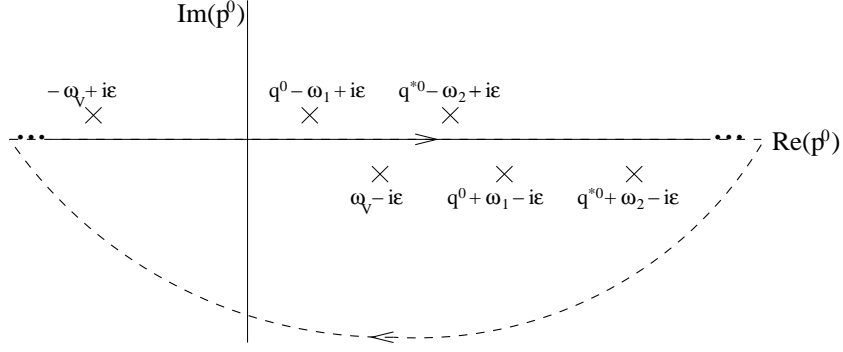


Figure 20: Poles and path for the evaluation of the P^0 integral.

$$\begin{aligned}
\tilde{A}_0 &= 2q^0 q^{*0} \omega_1 \omega_2 \omega_V - \omega_2 (\omega_2 + \omega_V) \left[\omega_1 (\omega_1 + \omega_2) (\omega_1 + \omega_V) - q^{*02} (\omega_1 + \omega_2 + \omega_V) \right] + \\
&\quad + q^{02} \left[-q^{*02} (\omega_1 + \omega_2) + \omega_1 (\omega_1 + \omega_V) (\omega_1 + \omega_2 + \omega_V) \right] \\
\tilde{A}_1 &= |\vec{P}| \cos \theta \left\{ -q^{02} q^{*02} \omega_2 + q^{*0} \omega_2 (\omega_2 + \omega_V) (2\omega_1 + \omega_2 + \omega_V) + \right. \\
&\quad \left. + q^0 \omega_1 \left[-q^{*02} + (\omega_1 + \omega_V) (\omega_1 + 2\omega_2 + \omega_V) \right] \right\} \\
\tilde{A}_a &= \frac{\vec{P}^2 \sin^2 \theta}{2\omega_V} \left\{ 2q^0 q^{*0} \omega_1 \omega_2 - q^{02} \omega_2 (\omega_1 + \omega_V) + \right. \\
&\quad \left. + (\omega_2 + \omega_V) \left[-q^{*02} \omega_1 + (\omega_1 + \omega_2) (\omega_1 + \omega_V) (\omega_1 + \omega_2 + \omega_V) \right] \right\} \\
\tilde{A}_b &= \tilde{A}_a \frac{(3 \cos^2 \theta - 1)}{\sin^2 \theta}
\end{aligned}$$

References

- [1] A. Bramon, G. Colangelo, P. J. Franzini and M. Greco, Phys. Lett. B **287** (1992) 263.
- [2] P. J. Franzini, W. Kim and J. Lee-Franzini, Phys. Lett. B **287** (1992) 259.
- [3] G. Colangelo and P. J. Franzini, Phys. Lett. B **289** (1992) 189.
- [4] N. N. Achasov, V. V. Gubin and E. P. Solodov, Phys. Rev. D **55** (1997) 2672 [arXiv:hep-ph/9610282].
- [5] A. Bramon, A. Grau and G. Pancheri, Phys. Lett. B **289** (1992) 97.
- [6] A. Bramon, R. Escribano, J. L. Lucio M, M. Napsuciale and G. Pancheri, Eur. Phys. J. C **26** (2002) 253 [arXiv:hep-ph/0204339].

- [7] E. Marco, S. Hirenzaki, E. Oset and H. Toki, Phys. Lett. B **470** (1999) 20 [arXiv:hep-ph/9903217].
- [8] Proc. of the Workshop on the "Possible existence of the σ meson and its implication in hadron physics", Kyoto June, 2000, Ed. S. Ishida et al., web page <http://amaterasu.kek.jp/YITPws/>.
- [9] J. A. Oller and E. Oset, Nucl. Phys. A **620** (1997) 438 [Erratum-ibid. A **652** (1999) 407] [arXiv:hep-ph/9702314].
- [10] J.A. Oller, E. Oset and J. R. Peláez, Phys. Rev. Lett. **80** (1998) 3452; *ibid*, Phys. Rev. D **59** (1999) 74001.
- [11] J. A. Oller and E. Oset, Phys. Rev. D **60** (1999) 074023 [arXiv:hep-ph/9809337].
- [12] J. L. Lucio Martinez and J. Pestieau, Phys. Rev. D **42** (1990) 3253.
- [13] F. E. Close, N. Isgur and S. Kumano, Nucl. Phys. B **389** (1993) 513 [arXiv:hep-ph/9301253].
- [14] A. Bramon, R. Escribano, J. L. Lucio M, M. Napsuciale and G. Pancheri, Eur. Phys. J. C **26** (2002) 253 [arXiv:hep-ph/0204339].
- [15] M. N. Achasov *et al.*, Phys. Lett. B **485** (2000) 349 [arXiv:hep-ex/0005017].
- [16] R. R. Akhmetshin *et al.* [CMD-2 Collaboration], Phys. Lett. B **462** (1999) 380 [arXiv:hep-ex/9907006].
- [17] M. N. Achasov *et al.*, Phys. Lett. B **479** (2000) 53 [arXiv:hep-ex/0003031].
- [18] A. Aloisio *et al.* [KLOE Collaboration], Phys. Lett. B **537** (2002) 21 [arXiv:hep-ex/0204013].
- [19] A. Aloisio *et al.* [KLOE Collaboration], Phys. Lett. B **536** (2002) 209 [arXiv:hep-ex/0204012].
- [20] P. Singer, Phys. Rev **128** (1962) 2789;
Phys. Rev **130** (1963) 2441; **161** (1967) 1694(E).
- [21] A. Bramon, A. Grau and G. Pancheri, Phys. Lett. B **283**, 416 (1992).
- [22] A. Bramon, R. Escribano, J. L. Lucio Martinez and M. Napsuciale, Phys. Lett. B **517** (2001) 345 [arXiv:hep-ph/0105179].
- [23] J. E. Palomar, S. Hirenzaki and E. Oset, Nucl. Phys. A **707** (2002) 161 [arXiv:hep-ph/0111308].
- [24] M. N. Achasov *et al.*, JETP Lett. **71**, 355 (2000) [Pisma Zh. Eksp. Teor. Fiz. **71**, 355 (2000)].

- [25] N. N. Achasov and A. V. Kiselev, arXiv:hep-ph/0212153.
- [26] N. N. Achasov and V. N. Ivanchenko, Nucl. Phys. B **315** (1989) 465.
- [27] M. Boglione and M. R. Pennington, arXiv:hep-ph/0303200.
- [28] K. Huber and H. Neufeld, Phys. Lett. B **357** (1995) 221 [arXiv:hep-ph/9506257].
- [29] G. Ecker, J. Gasser, A. Pich and E. de Rafael, Nucl. Phys. B **321** (1989) 311.
- [30] J. A. Oller, Phys. Lett. B **426** (1998) 7 [arXiv:hep-ph/9803214].
- [31] J. A. Oller, E. Oset and J. E. Palomar, Phys. Rev. D **63** (2001) 114009 [arXiv:hep-ph/0011096].
- [32] R. Urech, Phys. Lett. B **355** (1995) 308 [arXiv:hep-ph/9504238].
- [33] N.N. Achasov *et al.*, Int. J. Mod. Phys. A7 (1992) 3187, N.N. Achasov and A.A. Kozhevnikov, Phys. Lett. B233, (1989) 474 and Int. J. Mod. Phys. A7, (1992) 4825.
- [34] A. Bramon, R. Escribano and M. D. Scadron, Eur. Phys. J. C **7** (1999) 271 [arXiv:hep-ph/9711229].
- [35] A. Bramon, private communication
- [36] E. Oset, J. R. Pelaez and L. Roca, Phys. Rev. D **67** (2003) 073013 [arXiv:hep-ph/0210282].
- [37] K. Hagiwara *et al.* [Particle Data Group Collaboration], Phys. Rev. D **66** (2002) 010001.
- [38] J. A. Oller and E. Oset, Nucl. Phys. A **629** (1998) 739 [arXiv:hep-ph/9706487].
- [39] V. Bernard, N. Kaiser and U. G. Meissner, Phys. Rev. D **44** (1991) 3698.
- [40] R. Barbieri, R. Gatto and Z. Kunszt, Phys. Lett. B **66** (1977) 349.
- [41] R. K. Carnegie, R. J. Cashmore, W. M. Dunwoodie, T. A. Lasinski and D. W. Leith, Phys. Lett. B **68** (1977) 287.
- [42] M. Suzuki, Phys. Rev. D **47** (1993) 1252.
- [43] L. Roca, J. E. Palomar and E. Oset, arXiv:hep-ph/0306188.
- [44] J. A. Oller, Nucl. Phys. A **714** (2003) 161 [arXiv:hep-ph/0205121].
- [45] S. Giovanella and S. Miscetti, KLOE note 178
- [46] J. A. Oller, E. Oset and A. Ramos, Prog. Part. Nucl. Phys. **45** (2000) 157 [arXiv:hep-ph/0002193].